



Published in final edited form as:

*Wiley Interdiscip Rev Nanomed Nanobiotechnol.* 2015 March ; 7(2): 152–168. doi:10.1002/wnan.1314.

## Plasmonic Biosensors

**Ryan T. Hill**

Department of Biomedical Engineering, Duke University, Durham, NC, USA

Ryan T. Hill: ryan.hill@duke.edu

### Abstract

The unique optical properties of plasmon resonant nanostructures enable exploration of nanoscale environments using relatively simple optical characterization techniques. For this reason, the field of plasmonics continues to garner the attention of the biosensing community. Biosensors based on propagating surface plasmon resonances (SPRs) in films are the most well-recognized plasmonic biosensors, but there is great potential for the new, developing technologies to surpass the robustness and popularity of film-based SPR sensing. This review surveys the current plasmonic biosensor landscape with emphasis on the basic operating principles of each plasmonic sensing technique and the practical considerations when developing a sensing platform with the various techniques. The “gold standard” film SPR technique is reviewed briefly, but special emphasis is devoted to the up-and-coming LSPR-based and plasmonically coupled sensor technology.

### Introduction

Plasmonic biosensors can be roughly divided into two classes of sensing platforms: those that use thin metallic films and those that use individual inorganic plasmon resonant nanostructures. Within each class there are many sensing modalities and also there are examples of sensing platforms that combine both classes of sensors. By far the most widely used type of plasmonic biosensor is known to most people simply as “surface plasmon resonance” (SPR), a film based sensor, and has become the “gold standard” for characterizing interactions between biomolecules. However, the spectrum of the types of sensing that can be done with individual plasmon resonant nanostructures, even in combination with film-based sensing, is very diverse. New developments in these types of sensors show promise in terms of delivering the next “gold standard” plasmonic biosensor to market. The focus of this review will not be on figures of merit such as limit of detection and sensitivity —most plasmonic biosensors do not struggle with these— but rather the focus is on the types of plasmonic sensors that have been shown recently and the challenges associated implementing with them into robust sensing platforms. This is of interest because for as much excitement that is generated from plasmonics (*i.e.*, “nanohype”<sup>1</sup>), there are surprisingly few examples of robust plasmonic sensors that have passed the commercialization test.

### PROPAGATING SURFACE PLASMONS

Propagating plasmonic sensors are those that rely on the surface plasmons –collective oscillations of free surface electrons– supported by thin (~50 nm) metallic films. The most common metal film used is gold because it produces SPRs that can be interrogated using

visible wavelengths of light, it is a relatively inert metal (not prone to oxidation), and it can be easily functionalized with molecular linkers through favorable gold-thiol interactions or through adsorption. Excitation of the SPR in the film can be done in several ways, with the most common being the so-called Kretschmann configuration<sup>2, 3</sup> where light is coupled into the gold film by a glass prism that facilitates total internal reflection (TIR) of the input beam at the gold film/air interface (Figure 1a). Though there are other configurations that can excite film SPRs, in all instances a light coupling mechanism is necessary to match the momentum of the incoming photons to the free surface electrons of the gold film and create a SPR. This requirement of film based SPR studies has advantages and disadvantages. The advantage, particularly for the Kretschmann configuration is that the optical path of the sensing platform is totally contained on the backside of the sensor surface, which facilitates the use of flow cells on top of the sensor surface. The disadvantage is the fact that the prism can be a bulky and otherwise difficult optic to incorporate into compact, miniaturized sensing systems.

Film SPR experiments can be classified as angle-resolved or wavelength-resolved SPR, and are differentiated by the type of source used and hence the type of data that is gathered. In angle-resolved SPR the source is a laser, which provides illumination at a single wavelength. In this case the film SPR is detected by scanning the laser illumination angle to find the angle at which the light couples into the film and excites the SPR. Wavelength-resolved SPR is done with a broadband, white light source at a fixed angle, and the monitored sensor signal is the wavelength at which the SPR occurs at the given illumination angle. Both types of SPR produce a strong film SPR peak (Figure 1b), the location of which—either in angle or in wavelength—is tracked over time to indicate changes in the SPR of the film due to the particular sensing mechanism at hand. The SPR peak is seen in raw data as a minimum in the reflected light intensity from the standpoint of the detector, because at the SPR angle or wavelength, light transmission through the TIR optical path is being lost via coupling into the surface plasmons of the film.

The basis of the film SPR sensing mechanism is the fact that the SPR is highly sensitive to the refractive index (RI) of the medium in direct contact with the metal film, which in the case of biosensing is usually an aqueous solution (water, buffer, etc.). Because the SPR sensitivity to RI only extends ~200 nm into solution,<sup>4</sup> SPR sensing is an interfacial sensing technique, meaning that it only detects RI changes that happen close to the metal film surface. The most common sensing SPR sensing experiment is one where a receptor (antibody, aptamer, drug target, etc.) is first immobilized to the film surface using attachment chemistry or physisorption, preferably in a way that does not alter the binding properties of the molecule being immobilized (Figure 1c). After immobilization of this first molecular layer, a baseline response of the SPR instrument is determined, and then the change in the SPR location is monitored over time as a target analyte is introduced, usually via a flow cell, to the functionalized film surface. The SPR response over time (Figure 1d) can be used to determine kinetic parameters of the binding interaction, such as the association and dissociation constants for the receptor-target pair.<sup>4-6</sup> This use of film SPR for biosensing is perhaps the most widespread type of plasmonic biosensing due to the fact that the technology was incorporated into fairly robust, commercially available instruments. Now it is common to find SPR modules meant to interface with commercial ellipsometry

instruments as well. An important advantage of film SPR studies is the fact that the binding interactions can be studied in a label-free format, meaning that once the capture molecule is immobilized onto the sensor surface, no modifications (*i.e.* addition of fluorescent tags, etc.) are necessary to detect binding events that occur on the surface.

Anyone involved in film based SPR biosensing should consider the reviews by Rich and Myszka<sup>5-19</sup> as “must read” material. In a heroic effort, they published annual reviews of all film-based SPR biosensor research (~1000 articles per year) for over a decade (1999 – 2011) during the explosive growth period of SPR. The focus of their reviews is not merely to point out who did what, but to quite humorously educate the field as to how to properly conduct SPR biosensor experiments and analyze the resulting data. Reading through their annual reviews, it becomes apparent that their frustration mounted over time due to what they perceived as poor quality research being published. As a result, towards the end of their tenure they began grading the papers,<sup>18</sup> which makes for an interesting read. Regardless, these reviews point out many examples in the literature of the use of propagating SPRs in films to study binding interactions between receptor-target pairs (antibody/antigen, nucleic acid binding, etc.) and also more general molecular interaction data between molecules of interest (protein-nucleic acid, protein-lipid, cell-ligand, etc.). Furthermore, the review by Gopinath points out many examples of the types of biomolecular interactions typically probed with SPR, including a table of dissociation constants determined using SPR.<sup>20</sup>

Though film SPR is a widely established, robust, and commercially available tool for studying interfacial phenomena, the instrumentation required for film SPR analysis can be considered bulky from the standpoint of miniaturized sensing devices. This is due to the optics required to couple light into the metal film to excite the SPR, the need for temperature control to produce stable SPR signal, and also to the propagation length of the film SPR laterally on the film surface (from a few to hundreds of micrometers,<sup>21</sup>), which sets the lower limit on the size of the sensor surface.<sup>21</sup> For these reasons, it is generally difficult to incorporate film SPR sensors into small, portable, and multiplexed sensing devices that would perform in a lab-on-a-chip setting. That said, however, film SPR studies can exist in a multiplexed format by virtue of multichannel SPR instrument or SPR imaging. In SPR imaging,<sup>4, 22, 23</sup> receptor molecules can be patterned onto a film surface and then SPR imaging can be used to detect binding events from the patterned array, similar to what is accomplished by microarrays that detect binding via fluorescence.

## LOCALIZED SURFACE PLASMONS

Aside from propagating film-based SPR sensing, the other main category of plasmonic sensing is the use of localized surface plasmon resonances (LSPRs). As is the case in nanoscale thin metal films, metal nanostructures that are significantly smaller than the wavelength of incident light upon them can exhibit a SPR, or collective oscillation of the free surface electrons in response to the oscillating electric field of the light. When SPRs are excited in nanoscale 3D objects, such as nanoparticles (NPs), the SPRs are confined by the nanoscale objects, and hence are called LSPRs. Given that LSPR signal is generated from nanoscale objects, LSPR sensing platforms are more amenable to multiplexing and miniaturization than film SPR sensing platforms. This makes LSPR plasmonic sensors an

attractive option for incorporation into miniaturized lab-on-a-chip or point-of-care diagnostic devices. LSPRs of nanoscale objects can be tuned by varying the size, shape, and composition of the NPs.<sup>24, 25</sup> This is advantageous for sensing in biological samples because detection systems can be tuned to use wavelengths that do not overlap with the spectral features of strongly absorbing naturally occurring biological chromophores, such as hemoglobin in blood samples, to improve sensitivity to target analytes. Most LSPR sensors are designed to be RI sensors (Figure 2), analogous to film SPR sensors, however in some cases the LSPRs from plasmon resonant nanostructures are more simply used as visual tags as an alternative to fluorophore tags, or in some cases as therapeutic agents for cancer treatment. Several applications of LSPRs are described in the following subsections.

### Single Nanoparticle Localized Surface Plasmon Resonance Sensors

Single plasmon resonant NPs absorb and scatter incident light at their characteristic LSPR wavelength, which depends on the size, shape, and composition of the NP and also on the dielectric properties of the surrounding medium.<sup>25</sup> The scattering of the LSPR is bright enough that dark field microscopy can be used to identify single plasmon resonant NPs.<sup>25</sup> Though the resolution of optical microscopes is not high enough to image the true size of the plasmon resonant NPs, the color of the scattering from the NPs, or the LSPR wavelength, can be used to transduce changes in RI that are happening near the surface of the NPs<sup>26, 27</sup> (Figure 2). LSPR sensors are similar to film SPR sensors in that they are very sensitive to the RI of the surrounding medium, however, LSPR sensors have dramatically reduced sensing volumes<sup>21, 28</sup> and produce more localized sensor information. This is due to the fact that the LSPRs extend only tens of nanometers into the surrounding medium as opposed to hundreds of nanometers in the case of propagating film SPRs.<sup>28</sup> This reduced sensing volume extends the detection limit of single NP LSPR sensors to the single molecule level<sup>29</sup> (Figure 3), however, care must be taken when developing such sensing experiments to ensure that the binding of target molecule actually happens within the sensing volume as opposed to outside of it. This is a concern especially when the strategy to link receptors to the NP sensors involves bulky molecules.

Single NP LSPR sensing experiments are often designed similarly to film SPR sensing experiments, where a receptor molecule is immobilized to plasmon resonance NPs and then changes in the spectra of the NPs are monitored over time as the receptor molecules bind targets in solution.<sup>30–32</sup> Other examples of single NP LSPR sensing include monitoring nuclease activity on DNA-coated gold NPs<sup>33</sup> and also the development of a plasmonic enzyme-linked immunosorbent assay (ELISA) where enzymes immobilized to NPs catalyze a precipitation reaction on the surface of the NPs, which causes a detectable shift in the LSPR of the NPs.<sup>33</sup>

Though single NP LSPR sensors approach single molecule sensitivity, are label free, and perform similarly to the “gold standard” film SPR platform, the largest drawback of their use is the cumbersome nature of their experimental setup. In most cases a dark field microscope with attached spectrometer is required, and also interrogation of the single NPs is usually done one-by-one (though this is improving with various optical and imaging

techniques<sup>29, 33–35</sup>), so it becomes time consuming to gather enough data for statistical relevance in high-throughput.

### Ensemble Localized Surface Plasmon Resonance Sensors

Perhaps one of the most robust forms of LSPR sensing is transmission LSPR spectroscopy (T-LSPR) or some variant of the technique (Figure 4a). The sensor behaves similarly to a film SPR and single NP LSPR sensors, in that changes in a SPR with changes in refractive index are monitored. Similar to single NP LSPR sensors, T-LSPR signal is produced from very localized sensing volumes near the surfaces of the nanostructures, but instead of only probing one NP at a time, T-LSPR probes hundreds – millions at a time, which makes it a much higher throughput sensing platform. In contrast to film SPR sensors, T-LSPR sensors do not require extensive temperature control for stable signal output due to the smaller sensing volume of NP LSPRs. In its basic form, the T-LSPR sensor is comprised of a high density of plasmon resonant nanostructures immobilized onto a glass slide or similar transparent substrate (Figure 4b). The structures are typically in the form of colloidal NPs immobilized onto the substrate,<sup>36, 37</sup> island-like structures from annealed thin gold films,<sup>38–41</sup> or from nanostructures formed on the substrate by a patterning process.<sup>42–47</sup> The collective LSPR of a large population of the immobilized nanostructures are then interrogated in high throughput by a single optical extinction measurement (loss of light due to absorbance and scattering from the LSPRs) using a simple, collinear optical light path. This configuration is much more convenient than having to use specialized microscopy equipment, as is the case for single NP LSPR studies. In fact most T-LSPR studies are done using standard spectrophotometers, instruments that are ubiquitous in laboratory settings these days, by inserting the ensemble LSPR sensor surfaces into spectrophotometer cuvettes for LSPR measurements.<sup>36, 37, 40</sup> More recent work has demonstrated the ability to do multiplexed T-LSPR<sup>38, 42</sup> (Figure 4c), which should encourage more widespread use of T-LSPR sensors. The success of T-LSPR sensing is perhaps validated by the fact that there are commercial T-LSPR sensing platform available (LamdaGen, Insplorion). A notable variant of T-LSPR where ensembles of immobilized nanostructures are interrogated using high-throughput optical measurements are those done in a reflected optical geometry (*e.g.*, NPs immobilized on paper<sup>48</sup> and also on reflective metal film<sup>49, 50</sup>).

### Plasmon Resonant Nanoparticles as Labels

Plasmon resonant NPs are also commonly used as visual labels in sensing assays in similar ways as fluorophores are used, as it is straightforward to conjugate gold and silver NPs to biomolecules of interest.<sup>51</sup> The LSPRs of plasmon resonant NPs produce extremely large scattering cross-sections, and hence can be considered in some ways superior to commonly used fluorophore-based visualization in many types of sensing assays. The scattering from plasmon resonant NPs is not susceptible to photodegradation over time, as are fluorophores, and so degradation of signal with extended illumination time when using plasmon resonant NPs as tags is not a concern.<sup>51, 52</sup>

As discussed above, the scattering from plasmon resonance NPs can be so bright that single NPs can be seen using dark field microscopy, a feature that has been used to create a sensitive immunoassay similar to an ELISA called a plasmon-resonant immunosorbent

assay (PRISA).<sup>52</sup> This PRISA differs from the plasmonic ELISA described above in the single NP LSPR section in that the sensing mechanism is not based on changes in RI near the NPs. Here, NPs are linked to antibodies and simply serve as a bright, unbleachable optical tag to indicate target binding by establishing a relationship between the number of NPs immobilized to a sensor surface by the assay and the target concentration.

It is also possible to visualize ensembles of NPs by eye, which makes their use as tags applicable to sensing assays where simple visual readout is accomplished without magnification optics or filters. Many strategies have been reported for colorimetric visual-readout sensors using plasmon resonant NPs as tags,<sup>53–55</sup> but perhaps the most common and successful example is the lateral flow assay<sup>56, 57</sup> (e.g. a pregnancy test). These work by first depositing a sample solution onto a chromatographic membrane strip, after which the sample flows via capillary action through a region of the membrane containing antibody-labeled NPs. These NPs are carried with the sample solution to a region further along on the membrane strip that contains immobilized secondary antibody for the antigen of interest (Figure 5a). When antigen is present in the sample solution a dark line appears on the strip in a pre-determined location due to immobilization of the plasmon resonant NPs. The result can be a simple “yes/no” indication of the presence of an analyte, or in some cases it can be semi-quantitative (Figure 5b). These colorimetric detection schemes using plasmon resonant NPs make for extremely cost effective, easy-to-use diagnostic tests. A drawback is that it can be challenging to get good, quantitative data from visual-only detection. This can be improved by using imaging or simple spectroscopy techniques to quantify scattering intensity.

### Plasmon Resonant Nanoparticles Cancer Therapeutics

Plasmon resonant NPs are also implemented in cancer therapy techniques.<sup>58</sup> Since NPs are easily conjugated to biomolecules of interest and, in the case of gold NPs in particular, are considered to be fairly inert and biocompatible, their use in targeting cancer cells has been explored. Plasmonic photodynamic therapy is an example where plasmon resonant NPs are localized to cancerous tumor cells and then are heated, by virtue of absorption of illumination light at their LSPR wavelength, to an extent that the excess heat promotes cancer cell death.<sup>59–62</sup> In other cases the NPs are used as carriers of drug molecules (such as silencing RNA<sup>63</sup>) to tumor cells to inhibit tumor cell growth. Once NPs are localized to tumor cells, the drugs conjugated to their surface can be released by intense illumination at the NP LSPR wavelength and subsequently promote cell death within the tumor.<sup>63</sup> Plasmon resonant NPs are also used to enhance various types of biomedical imaging techniques for *in vitro* cancer studies. This topic is detailed more in depth in a separate *WIREs Nanomedicine & Nanobiotechnology* review article by Tuan Vo-Dinh.<sup>64</sup>

### PLASMONIC NANOPORES

The use of plasmonic nanopores in thin metal films for sensing combines characteristics of propagating SPR and LSPR sensing. Plasmonic nanopore sensing is based on the extraordinary optical transmission (EOT) that exists when nanopore arrays are illuminated, an effect that arises from the excitation of plasmonic modes defined by the grating orders of the pore array.<sup>65</sup> The EOT can serve as a sensor by either monitoring the intensity changes of light

passing through pores<sup>66</sup> or by monitoring shifts in the spectrum of the light transmitted through the pores, as the spectra are sensitive to the size/shape of the pores, the dimensions of the pore array, and also to any changes in the local refractive index<sup>67</sup> (*e.g.*, target binding events,<sup>68</sup> Figure 6d–f) that occur near or in the pores. Since the pores are nano-sized plasmonic features, they can also exhibit LSPRs with RI sensitivity as described above and hence can be used similarly to LSPR RI sensors.<sup>69, 70</sup>

Sensing with plasmonic nanopores is one of the most exciting plasmonic prospects for incorporation into miniaturized, self-contained sensing devices<sup>65</sup> (Figure 6b and 6c) several reasons. First, pores can be interrogated with a simple collinear optical configuration with few optics,<sup>65</sup> and hence instrumentation required does not have to be complex. Second, pores are nano-sized, which means that they align well with miniaturized detection systems that can support multiplexing,<sup>71</sup> because many dense nanopore arrays can be integrated into small, chip-sized sensors. Third, nanopore arrays are fairly easy to create with standard patterning processes. Fourth, the use of pores as a sensing element enables flow-through studies<sup>72</sup> that can improve limits of detection in cases where sensing is otherwise mass-transport limited. This is especially important for detection of extremely low concentration analytes. Flow through studies also enable the interrogation membranes suspended over the pores, such as lipid bilayers containing membrane proteins.<sup>73</sup>

## PLASMON COUPLING

Another major class of plasmonic biosensors makes use of plasmon coupling to transduce sensing output. When surface plasmon supporting surfaces are in close proximity to each other (typically less than ~50 nm), their surface plasmons can become coupled, which dramatically impacts the spectral signature from the surfaces.<sup>74</sup> This section discusses the various ways in which plasmonic coupling can be used for biosensing.

### Plasmonically Coupled Nanoparticle Assemblies as Plasmon Rulers

A classic example of plasmon coupling in sensing is the use of the plasmon ruler to detect DNA. To do so, two plasmon resonant NPs are first linked together using single stranded or hairpin DNA<sup>75–77</sup> to create a NP dimer (Figure 7a), which displays a dramatically red-shifted, plasmonically coupled LSPR relative to that of the individual NP LSPRs. If the separation distance between the NPs is increased by a stimulus, the coupled LSPR blue shifts in a distance-dependent manner. This effect is used to detect DNA by subjecting the single stranded DNA-linked NP dimers to a DNA target complementary to the DNA NP linker, and as the DNA strands hybridize the separation distance between the NPs increases due to the increased persistence length and rigidity of the double stranded DNA. This separation is detected as a blue shift from an individual NP dimer, visualized using dark field microscopy (Figure 7b). Since the initial demonstration of a DNA linked plasmon ruler<sup>75</sup> the concept of the plasmon ruler has been well-studied both experimentally and theoretically,<sup>78–83</sup> and so it is possible to precisely calibrate the distance dependent LSPR shifts with NP separation distance, which enables the use of plasmon rulers as metrology sensors.

Plasmon rulers are attractive as sensors because they can achieve Angstrom scale, atomic bond length distance sensitivity,<sup>84</sup> which can be exploited similarly to Förster Resonance Energy Transfer (FRET) based sensors where subtle molecular structural changes can be detected. The advantages of plasmon rulers over FRET rulers are that plasmon ruler signal output arises from bright plasmonic scattering that does not photobleach as do fluorophores<sup>52</sup> and also that plasmon rulers can be tuned for distance sensitivity spanning greater distances than is possible with FRET rulers.<sup>75</sup> Also, an advantage of plasmon rulers over SPR and LSPR sensors described in the previous sections is their potential for increased sensitivity to small molecules, which would pose a problem for LSPR and SPR sensors due to their small impact on local RI, but would be easily detected as a distance change by plasmon rulers.

The largest challenge to using plasmon rulers in sensing platforms is developing efficient ways to reliably fabricate the plasmon rulers and also to characterize their sensor output signal in high throughput. Assemblies of plasmon resonant NPs, where many NPs are linked together, can be used as plasmon ruler sensors and can be fabricated fairly efficiently in solution using self-assembly via molecular linkers.<sup>85–89</sup> These plasmon rulers can be characterized in high throughput using ensemble optical measurements or colorimetric detection by eye, but their utility in biosensing is limited by the fact that colloidal solutions easily destabilize with changes in salt concentration or the addition of other biomolecules such as protein or DNA. Though salt induced flocculation of colloidal solutions has been used successfully for colorimetric detection of proteins and cells,<sup>90</sup> this issue of stability makes it challenging to use colloidal assemblies in direct contact with biological fluids like serum or blood.

A way to avoid colloidal flocculation with plasmon ruler sensors is to immobilize them onto substrates, after which the substrates can be exposed to biological samples and the plasmon rulers remain stable and active as sensors. This can be done by first creating the plasmon ruler assemblies in solution<sup>91</sup> and optionally purifying them<sup>83, 92, 93</sup> before immobilizing them, or by building the plasmon ruler assemblies using a bottom-up process whereby stabilized single NPs are first immobilized to the surface, then functionalized to bind a second set of NPs, and then exposed to the second set of NPs to create surface bound plasmon rulers.<sup>75–77, 94–96</sup> Both methods suffer from low plasmon ruler fabrication efficiency and often times the result is that individual plasmon rulers must be identified one-by-one among a large background population of single NPs or unwanted NP aggregates using a dark field microscope.<sup>77, 78</sup> This can limit the throughput of the sensor because it becomes cumbersome to build a set of data from a large population of active plasmon rulers. That said, however, there are examples of successful sensors where high-throughput ensemble measurements are made from coupled NP assemblies (*e.g.* detection of protease activity<sup>96</sup> and polymer swelling<sup>97, 98</sup>). These cases typically do not transduce accurate distance changes between the plasmon ruler reporters because of the heterogeneity of the sensor fabrication, but through plasmon coupling they transduce meaningful sensor data nevertheless. Furthermore, NP dimer and NP assembly plasmon rulers immobilized onto substrates have been used in other studies, despite the disadvantages in fabrication efficiency and throughput, to successfully detect DNA<sup>75–77, 95, 99</sup> and protein<sup>94</sup>; and to monitor



molecular structural changes<sup>92</sup> and ribonuclease activity.<sup>93</sup> Plasmon rulers are also being incorporated into a specialized imaging technique called plasmon coupling microscopy,<sup>100</sup> which has been used to study expression levels of proteins on cell surfaces.<sup>101, 102</sup>

### Film Coupled Nanoparticles as Plasmon Rulers

In addition to surface plasmon coupling between NPs, it is also possible for NP localized surface plasmons to couple to surface plasmons supported by nearby thin metallic film. In this case the film (usually gold or silver) serves to create an image dipole (analogous to a mirror reflection, Figure 8a) that recapitulates the effect of two “real” metal NPs that are physically separated in space.<sup>103</sup> Similar to the case of coupled NP-dimers, this NP-film coupling mechanism can also act as a plasmon ruler.<sup>84, 103–108</sup> This was demonstrated by creating increasingly thick molecular layers on the gold film (Figure 8b), onto which gold NPs were deposited. The LSPRs of the NPs blue shifted dramatically as the NP-film separation distance increased (Figures 8c and 8d).

The NP-film plasmon ruler has potential advantages over the NP dimer/assembly plasmon rulers described in the section above, because NP-film plasmon rulers are created with 100% yield (Figures 8e–h) by a simple process of depositing NPs onto the film using a molecular spacer layer that typically is formed on the film beforehand. This fabrication process is capable of creating billions of identical plasmon rulers over very large surface areas (coverage of full microscope slides is easily accomplished). This high fabrication efficiency enables the use high-throughput optical measurements where millions of rulers are interrogated with a single optical measurement from a spectrophotometer,<sup>84, 105, 106, 108</sup> thus eliminating the need to identify and characterize rulers one-by-one using microscopy. The ability to use ensemble measurements increases the throughput, precision, and accuracy of the plasmon ruler sensor. As a result of these advantages of the NP-film plasmon ruler the extremes of plasmon coupling have been characterized<sup>84, 106</sup> by placing NPs extremely close to gold film (as close as 5 Angstroms) using ultrathin molecular spacer layers; a feat that remains challenging for NP dimer based plasmon rulers but is relatively simple to do with NP-film plasmon rulers. In this “extreme coupling” plasmon ruler regime, the plasmon ruler is capable of discerning distances on the order of atomic bond lengths by displaying a spectral shift of 5 nm for every 1 Angstrom change in distance.<sup>84</sup> The advantages of the NP-film plasmon ruler suggest that it will enable the development of more robust biosensors that utilize plasmon ruler technology.

### Film Coupled Nanoparticles for Enhanced Surface Plasmon Resonance

While the above discussion focuses on NP-film plasmonic coupling from the standpoint of the NP LSPR, it is also possible to take advantage of the coupling effect from the standpoint of the film SPR by interrogating the film SPR using TIR illumination, as described above in the Propagating Surface Plasmons section. This strategy is often called “enhanced SPR”<sup>109–111</sup> and involves immobilizing NPs to planar gold film to produce enhanced film SPR sensitivity to RI. Enhanced SPR has been used to detect the binding of target molecules,<sup>112, 113</sup> protein conformation changes,<sup>114, 115</sup> and polymer layer actuation.<sup>116</sup> In many instances of enhanced SPR, the film SPRs are interrogated in an angle-resolved SPR configuration using only a single wavelength, and hence it is sometimes unclear as to

whether the detected signal is from the film SPR, the NP LSPR, or a combination of the two. Recently the role of NP LSPRs in NP-film coupling responsible for enhanced SPR has been characterized.<sup>105</sup> This study showed that when using wavelength-resolved SPR at an optimal TIR illumination angle, it is possible to observe both the film SPR and the NP LSPR –two different sensor signals; the film SPR transducing RI and the NP LSPR being a plasmon ruler– in the same spectrum. The NP LSPR component of the spectrum was used to deduce distance changes between the NPs and film in response to an applied electric field, by virtue of the NP-film plasmon ruler effect. Additionally, Hong and Hall recently reported a nice study aimed at clarifying distance-dependence of the contribution of film coupled NPs to the enhancement of the film SPR signal.<sup>117</sup>

## FIELD ENHANCEMENTS

Another modality of plasmonic sensing arises from the fact that light incident on plasmon resonant nanostructures interacts with the LSPRs of the nanostructures to create very small regions near the nanostructure surface where electromagnetic fields become enhanced relative to the incident illumination. The magnitude of the enhancement depends on how tightly confined the enhanced fields are in space. For example, nanostructures with sharp corners<sup>118–120</sup> or nearly touching NP dimers<sup>121–123</sup> are known to create very large, highly localized field enhancements. These field enhancements can be large enough to stimulate surface enhanced Raman scattering<sup>124</sup> (SERS) —inelastic scattering from molecular vibrational modes— from molecules located within the field-enhanced region. This scattering contains chemically specific information that can be used to identify target molecules in samples,<sup>125, 126</sup> which is advantageous for sensing. However, it is more common to see SERS based sensors that track specific peaks in SERS spectra from known reporter molecules as the signal transduction mechanism. An example of such a mechanism is illustrated by Driskell *et al.*<sup>127</sup> in a manner similar to a sandwich immunoassay where a gold film is labeled with antibody that binds antigen, which is then labeled with gold NP that is conjugated to secondary antibody along with a Raman reporter. When antigen is present, the gold NP with Raman reporter binds to the gold film, which places the Raman reporter in a field-enhanced hot spot that enables spectral detection of its unique Raman signature.

SERS sensors are especially attractive because of the potential for chemically specific detection and because the enhanced fields can effectively improve limits of detection (single molecule detection is possible<sup>122, 128</sup>) and sensitivity, but SERS sensors are still limited by the difficulty in creating reproducible and uniform SERS hot spots, especially for miniaturized lab-on-a-chip type devices. Hot spots created by NP assemblies<sup>129</sup> or forced NP aggregation<sup>130–132</sup> are generally used to create hot spots, but these methods are fairly inefficient and uncontrollable in terms of producing a high yield of uniform hot spots. Interestingly, a SERS microfluidic device using salt induced aggregation to create SERS hot spots for drug detection in saliva was recently demonstrated.<sup>125</sup> Other examples of SERS sensors are tumor targeting and detection,<sup>133</sup> microRNA detection,<sup>126</sup> DNA detection,<sup>134, 135</sup> leukemia marker detection,<sup>136</sup> and immunoassays.<sup>137</sup>

A more uniform way to create field-enhanced uniform hot spots is to use the coupled NP-film platform described above.<sup>104, 138–146</sup> This platform offers an extremely high degree of

control over the separation distance between the NPs and film, even down to the Angstrom level, and so it is possible with this system to efficiently create large quantities of uniform hotspots. For example, electrostatically immobilizing gold NPs to a gold film using a thin molecular spacer layer resulted in a SERS hot spot in-between every film-coupled NP;<sup>104</sup> hot spot formation with 100% yield (Figure 9). This NP-film SERS platform has enabled various types of biosensing demonstrations, with a few examples being the detection of viral pathogens,<sup>147</sup> DNA,<sup>142</sup> antibody-antigen interactions,<sup>127</sup> adenosine,<sup>140</sup> and polymer actuation.<sup>139</sup>

SERS sensors remain an active topic in plasmonic biosensing as well as theranostics, photothermal therapy, and biomedical imaging applications. All of these topics are discussed in more detail in a related *WIREs Nanomedicine & Nanobiotechnology* review by Tuan Vo-Dinh.<sup>64</sup> Another related review by Punj *et al.*<sup>148</sup> discusses how plasmonically enhanced fields can enhance fluorescence for biosensing applications.

## Conclusion

The field of plasmonic biosensors remains innovative and continues to produce good prospects for robust sensing platforms. The propagating film SPR platform is perhaps still the most successful plasmonic sensing device to date, but the platforms being developed that utilize LSPRs for RI sensing are up-and-coming as their performance is now well-characterized and established. Newer sensing platforms being developed with plasmonic nanopore and plasmon coupling technologies also show a lot of promise. The nanopore platform has unique characteristics, such as the ability utilize flow-through studies and simple optical design, that make it especially well suited for miniaturized lab-on-a-chip devices. The plasmon coupling and field-enhanced technologies truly push the extremes of sensitivity for optical biosensors. The future of these technologies for sensing will likely depend on gaining control over the nanoscale assemblies so as to be able to tap into these sensitivity extremes with high efficiency. The overall outlook for new plasmonic biosensors remains positive; as these sensors have the unique ability to produce nanoscale, single molecule information using, in many cases, relatively simple and widely available optical instruments.

## Acknowledgments

This work was supported by grants from the NIH (R21HL115410) and NSF (1033621).

## References

1. Dahlin AB. Size matters: problems and advantages associated with highly miniaturized sensors. *Sensors*. 2012; 12:3018–3036. [PubMed: 22736990]
2. Homola J, Yee SS, Gauglitz G. Surface plasmon resonance sensors: review. *Sens Actuators B Chem*. 1999; 54:3–15.
3. Snopok B. Theory and Practical Application of Surface Plasmon Resonance for Analytical Purposes. *Theor Exp Chem*. 2012; 48:283–306.
4. Campbell CT, Kim G. SPR microscopy and its applications to high-throughput analyses of biomolecular binding events and their kinetics. *Biomaterials*. 2007; 28:2380–2392. [PubMed: 17337300]

5. Rich RL, Myszka D. Survey of the year 2007 commercial optical biosensor literature. *J Mol Recognit.* 2008; 21:355–400. [PubMed: 18951413]
6. Myszka D, Rich RL. Implementing surface plasmon resonance biosensors in drug discovery. *Pharm Sci Technol Today.* 2000; 3:310–317. [PubMed: 10996572]
7. Myszka D. Survey of the 1998 optical biosensor literature. *J Mol Recognit.* 1999
8. Rich RL, Myszka D. Advances in surface plasmon resonance biosensor analysis. *Curr Opin Biotechnol.* 2000; 11:54–61. [PubMed: 10679342]
9. Rich RL, Myszka D. Survey of the 1999 surface plasmon resonance biosensor literature. *J Mol Recognit.* 2000; 13:388–407. [PubMed: 11114072]
10. Rich RL, Myszka D. Survey of the year 2000 commercial optical biosensor literature. *J Mol Recognit.* 2001; 14:273–294. [PubMed: 11746948]
11. Rich RL, Myszka D. Survey of the year 2001 commercial optical biosensor literature. *J Mol Recognit.* 2002; 15:352–376. [PubMed: 12501157]
12. Rich RL, Myszka D. A survey of the year 2002 commercial optical biosensor literature. *J Mol Recognit.* 2003; 16:351–382. [PubMed: 14732928]
13. Rich RL, Myszka D. Why you should be using more SPR biosensor technology. *Drug Discov Today Technol.* 2004; 1:301–308. [PubMed: 24981499]
14. Rich RL, Myszka D. Survey of the year 2003 commercial optical biosensor literature. *J Mol Recognit.* 2005; 18:1–39. [PubMed: 15549676]
15. Rich RL, Myszka D. Survey of the year 2004 commercial optical biosensor literature. *J Mol Recognit.* 2005; 18:431–478. [PubMed: 16252250]
16. Rich RL, Myszka D. Survey of the year 2005 commercial optical biosensor literature. *J Mol Recognit.* 2006; 19:478–534. [PubMed: 17125150]
17. Rich RL, Myszka D. Survey of the year 2006 commercial optical biosensor literature. *J Mol Recognit.* 2007; 20:300–366. [PubMed: 18074396]
18. Rich RL, Myszka D. Grading the commercial optical biosensor literature—Class of 2008: ‘The Mighty Binders’. *J Mol Recognit.* 2009; 23:1–64. [PubMed: 20017116]
19. Rich RL, Myszka D. Survey of the 2009 commercial optical biosensor literature. *J Mol Recognit.* 2011; 24:892–914. [PubMed: 22038797]
20. Gopinath S. Biosensing applications of surface plasmon resonance-based Biacore technology. *Sens Actuators B Chem.* 2010
21. Brolo AG. Plasmonics for future biosensors. *Nat Photonics.* 2012; 6:709–713.
22. Nelson BP, Grimsrud TE, Liles MR, Goodman RM, Corn RM. Surface plasmon resonance imaging measurements of DNA and RNA hybridization adsorption onto DNA microarrays. *Anal Chem.* 2001; 73:1–7. [PubMed: 11195491]
23. Smith EA, Thomas WD, Kiessling LL, Corn RM. Surface plasmon resonance imaging studies of protein-carbohydrate interactions. *J Am Chem Soc.* 2003; 125:6140–6148. [PubMed: 12785845]
24. Mock JJ, Barbic M, Smith DR, Schultz DA, Schultz S. Shape effects in plasmon resonance of individual colloidal silver nanoparticles. *J Chem Phys.* 2002; 116:6755.
25. Anker J, Hall W, Lyandres O, Shah N, Zhao J, Van Duyne RP. Biosensing with plasmonic nanosensors. *Nat Mater.* 2008; 7:442–453. [PubMed: 18497851]
26. McFarland A, Van Duyne RP. Single silver nanoparticles as real-time optical sensors with zeptomole sensitivity. *Nano Lett.* 2003; 3:1057–1062.
27. Mock JJ, Smith DR, Schultz S. Local refractive index dependence of plasmon resonance spectra from individual nanoparticles. *Nano Lett.* 2003; 3:485–492.
28. Dahlin AB, Wittenberg NJ, Höök F, Oh S-H. Promises and challenges of nanoplasmonic devices for refractometric biosensing. *Nanophotonics.* 2013; 2:1–19.
29. Ament I, Prasad J, Henkel A, Schmachtel S, Sönnichsen C. Single unlabeled protein detection on individual plasmonic nanoparticles. *Nano Lett.* 2012; 12:1092–1095. [PubMed: 22268768]
30. Guo L, Zhou X, Kim D-H. Facile fabrication of distance-tunable Au-nanorod chips for single-nanoparticle plasmonic biosensors. *Biosens Bioelectron.* 2011; 26:2246–2251. [PubMed: 21035320]

31. Nusz GJ, Curry AC, Marinakos SM, Wax A, Chilkoti A. Rational selection of gold nanorod geometry for label-free plasmonic biosensors. *ACS Nano*. 2009; 3:795–806. [PubMed: 19296619]
32. Nusz GJ, Marinakos SM, Curry AC, Dahlin AB, Höök F, Wax A, Chilkoti A. Label-free plasmonic detection of biomolecular binding by a single gold nanorod. *Anal Chem*. 2008; 80:984–989. [PubMed: 18197636]
33. Chen S, Svedendahl M, Van Duyne RP, Käll M. Plasmon-enhanced colorimetric ELISA with single molecule sensitivity. *Nano Lett*. 2011; 11:1826–1830. [PubMed: 21428275]
34. Nusz GJ, Marinakos SM, Rangarajan S, Chilkoti A. Dual-order snapshot spectral imaging of plasmonic nanoparticles. *Appl Opt*. 2011; 50:4198–4206. [PubMed: 21772408]
35. Guo L, Ferhan AR, Lee K, Kim D-H. Nanoarray-based biomolecular detection using individual Au nanoparticles with minimized localized surface plasmon resonance variations. *Anal Chem*. 2011; 83:2605–2612. [PubMed: 21388163]
36. Marinakos SM, Chen S, Chilkoti A. Plasmonic detection of a model analyte in serum by a gold nanorod sensor. *Anal Chem*. 2007; 79:5278–5283. [PubMed: 17567106]
37. Nath N, Chilkoti A. A colorimetric gold nanoparticle sensor to interrogate biomolecular interactions in real time on a surface. *Anal Chem*. 2002; 74:504–509. [PubMed: 11838667]
38. Jia K, Bijeon JL, Adam PM, Ionescu RE. A facile and cost-effective TEM grid approach to design gold nano-structured substrates for high throughput plasmonic sensitive detection of biomolecules. *Analyst*. 2013; 138:1015–1019. [PubMed: 23304693]
39. Kedem O, Vaskevich A, Rubinstein I. Critical Issues in Localized Plasmon Sensing. *J Phys Chem C*. 2014; 118:8227–8244.
40. Kedem O, Tesler AB, Vaskevich A, Rubinstein I. Sensitivity and optimization of localized surface plasmon resonance transducers. *ACS Nano*. 2011; 5:748–760. [PubMed: 21226492]
41. Kalyuzhny G, Vaskevich A, Schneeweiss MA, Rubinstein I. Transmission surface-plasmon resonance (T-SPR) measurements for monitoring adsorption on ultrathin gold island films. *Chem Eur J*. 2002; 8:3849–3857. [PubMed: 12203279]
42. A imovi SS, Ortega MA, Sanz V, Berthelot J, Garcia-Cordero JL, Renger J, Maerkl SJ, Kreuzer MP, Quidant R. LSPR Chip for Parallel, Rapid, and Sensitive Detection of Cancer Markers in Serum. *Nano Lett*. 2014; 14:2636–2641. [PubMed: 24730454]
43. McPhillips J, McClatchey C, Kelly T, Murphy A, Jonsson MP, Wurtz G, Winfield R, Pollard RJ. Plasmonic Sensing Using Nanodome Arrays Fabricated by Soft Nanoimprint Lithography. *J Phys Chem C*. 2011; 115:15234–15239.
44. McPhillips J, Murphy A, Jonsson MP, Hendren WR, Atkinson R, Höök F, Zayats AV, Pollard RJ. High-performance biosensing using arrays of plasmonic nanotubes. *ACS Nano*. 2010; 4:2210–2216. [PubMed: 20218668]
45. Chen S, Svedendahl M, Käll M, Gunnarsson L, Dmitriev A. Ultrahigh sensitivity made simple: nanoplasmonic label-free biosensing with an extremely low limit-of-detection for bacterial and cancer diagnostics. *Nanotechnology*. 2009; 20:434015. [PubMed: 19801769]
46. Dahlin AB, Chen S, Jonsson MP, Gunnarsson L, Käll M, Höök F. High-resolution microspectroscopy of plasmonic nanostructures for miniaturized biosensing. *Anal Chem*. 2009; 81:6572–6580. [PubMed: 19621881]
47. Haes AJ, Van Duyne RP. A nanoscale optical biosensor: sensitivity and selectivity of an approach based on the localized surface plasmon resonance spectroscopy of triangular silver nanoparticles. *J Am Chem Soc*. 2002; 124:10596–10604. [PubMed: 12197762]
48. Parolo C, Merkoçi A. Paper-based nanobiosensors for diagnostics. *Chem Soc Rev*. 2013; 42:450–457. [PubMed: 23032871]
49. Kim D-K, Yoo SM, Park TJ, Yoshikawa H, Tamiya E, Park JY, Lee SY. Plasmonic Properties of the Multispot Copper-Capped Nanoparticle Array Chip and Its Application to Optical Biosensors for Pathogen Detection of Multiplex DNAs. *Anal Chem*. 2011; 83:6215–6222. [PubMed: 21714496]
50. Endo T, Kerman K, Nagatani N, Hiepa HM, Kim D-K, Yonezawa Y, Nakano K, Tamiya E. Multiple label-free detection of antigen-antibody reaction using localized surface plasmon resonance-based core-shell structured nanoparticle layer nanochip. *Anal Chem*. 2006; 78:6465–6475. [PubMed: 16970322]

51. Seydack M. Nanoparticle labels in immunosensing using optical detection methods. *Biosens Bioelectron.* 2005; 20:2454–2469. [PubMed: 15854819]
52. Schultz S, Smith DR, Mock JJ, Schultz DA. Single-target molecule detection with nonbleaching multicolor optical immunolabels. *Proc Natl Acad Sci U S A.* 2000; 97:996–1001. [PubMed: 10655473]
53. Zhou X, Xia S, Lu Z, Tian Y, Yan Y, Zhu J. Biomineralization-Assisted Ultrasensitive Detection of DNA. *J Am Chem Soc.* 2010; 132:6932–6934. [PubMed: 20441191]
54. Gupta S, Huda S, Kilpatrick PK, Velev OD. Characterization and optimization of gold nanoparticle-based silver-enhanced immunoassays. *Anal Chem.* 2007; 79:3810–3820. [PubMed: 17429944]
55. Taton TA. Scanometric DNA Array Detection with Nanoparticle Probes. *Science.* 2000; 289:1757–1760. [PubMed: 10976070]
56. Rong-Hwa S, Shiao-Shek T, Der-Jiang C, Yao-Wen H. Gold nanoparticle-based lateral flow assay for detection of staphylococcal enterotoxin B. *Food Chem.* 2010; 118:462–466.
57. Posthuma-Trumpie GA, Korf J, Amerongen A. Lateral flow (immuno)assay: its strengths, weaknesses, opportunities and threats. A literature survey. *Anal Bioanal Chem.* 2009; 393:569–582. [PubMed: 18696055]
58. Cai W, Gao T, Hong H, Sun J. Applications of gold nanoparticles in cancer nanotechnology. *Nanotechnol Sci Appl.* 2008; 1:17–32. [PubMed: 24198458]
59. Huang X, Jain PK, El-Sayed IH, El-Sayed MA. Plasmonic photothermal therapy (PPTT) using gold nanoparticles. *Lasers Med Sci.* 2008; 23:217–228. [PubMed: 17674122]
60. El-Sayed IH, Huang X, El-Sayed MA. Selective laser photo-thermal therapy of epithelial carcinoma using anti-EGFR antibody conjugated gold nanoparticles. *Cancer Lett.* 2006; 239:129–135. [PubMed: 16198049]
61. Loo C, Lowery A, Halas NJ, West JL, Drezek R. Immunotargeted nanoshells for integrated cancer imaging and therapy. *Nano Lett.* 2005; 5:709–711. [PubMed: 15826113]
62. Hirsch LR, Stafford RJ, Bankson JA, Sershen SR, Rivera B, Price RE, Hazle JD, Halas NJ, West JL. Nanoshell-mediated near-infrared thermal therapy of tumors under magnetic resonance guidance. *Proc Natl Acad Sci U S A.* 2003; 100:13549–13554. [PubMed: 14597719]
63. Huang X, Pallaoro A, Braun GB, Morales DP, Ogunyankin MO, Zasadzinski JA, Reich NO. Modular plasmonic nanocarriers for efficient and targeted delivery of cancer-therapeutic siRNA. *Nano Lett.* 2014.10.1021/nl500214e
64. Vo-Dinh T. SERS Nanosensors and Nanoreporters: Golden Opportunities in Biomedical Applications. *Wiley Interdiscip Rev Nanomed Nanobiotechnol.* 2014 Currently Under Review.
65. Cetin AE, Coskun AF, Galarreta BC, Huang M, Herman D, Ozcan A, Altug H. Handheld high-throughput plasmonic biosensor using computational on-chip imaging. *Light Sci Appl.* 2014; 3:e122.
66. Wang Y, Kar A, Paterson A, Kourentzi K, Le H, Ruchhoeft P, Willson R, Boa J. Transmissive Nanohole Arrays for Massively-Parallel Optical Biosensing. *ACS Photonics.* 2014; 1:241–245. [PubMed: 25530982]
67. Brolo AG, Gordon R, Leathem B, Kavanagh K. Surface plasmon sensor based on the enhanced light transmission through arrays of nanoholes in gold films. *Langmuir.* 2004; 20:4813–4815. [PubMed: 15984236]
68. Yanik AA, Huang M, Kamohara O, Artar A, Geisbert TW, Connor JH, Altug H. An Optofluidic Nanoplasmonic Biosensor for Direct Detection of Live Viruses from Biological Media. *Nano Lett.* 2010; 10:4962–4969. [PubMed: 21053965]
69. Dahlin AB, Zäch M, Rindzevicius T, Käll M, Sutherland DS, Höök F. Localized surface plasmon resonance sensing of lipid-membrane-mediated biorecognition events. *J Am Chem Soc.* 2005; 127:5043–5048. [PubMed: 15810838]
70. Jonsson MP, Jönsson P, Dahlin AB, Höök F. Supported lipid bilayer formation and lipid-membrane-mediated biorecognition reactions studied with a new nanoplasmonic sensor template. *Nano Lett.* 2007; 7:3462–3468. [PubMed: 17902726]

71. Lee SH, Lindquist NC, Wittenberg NJ, Jordan LR, Oh S-H. Real-time full-spectral imaging and affinity measurements from 50 microfluidic channels using nanohole surface plasmon resonance. *Lab Chip*. 2012; 12:3882. [PubMed: 22895607]
72. Eftekhari F, Escobedo C, Ferreira J, Duan X, Giroto EM, Brolo AG, Gordon R, Sinton D. Nanoholes As Nanochannels: Flow-through Plasmonic Sensing. *Anal Chem*. 2009; 81:4308–4311. [PubMed: 19408948]
73. Im H, Wittenberg NJ, Lesuffleur A, Lindquist NC, Oh S-H. Membrane protein biosensing with plasmonic nanopore arrays and pore-spanning lipid membranes. *Chem Sci*. 2010; 1:688. [PubMed: 21218136]
74. Su K, Wei Q, Zhang X, Mock JJ, Smith DR, Schultz S. Interparticle coupling effects on plasmon resonances of nanogold particles. *Nano Lett*. 2003; 3:1087–1090.
75. Sönnichsen C, Reinhard BM, Liphardt J, Alivisatos AP. A molecular ruler based on plasmon coupling of single gold and silver nanoparticles. *Nat Biotechnol*. 2005; 23:741–745. [PubMed: 15908940]
76. Chen JIL, Chen Y, Ginger DS. Plasmonic nanoparticle dimers for optical sensing of DNA in complex media. *J Am Chem Soc*. 2010; 132:9600–9601. [PubMed: 20583833]
77. Guo L, Ferhan AR, Chen H, Li C, Chen G, Hong S, Kim D-H. Distance-Mediated Plasmonic Dimers for Reusable Colorimetric Switches: A Measurable Peak Shift of More than 60 nm. *Small*. 2012; 9:234–240. [PubMed: 22930539]
78. Reinhard BM, Siu M, Agarwal H, Alivisatos AP, Liphardt J. Calibration of dynamic molecular rulers based on plasmon coupling between gold nanoparticles. *Nano Lett*. 2005; 5:2246–2252. [PubMed: 16277462]
79. Gunnarsson L, Rindzevicius T, Prikulis J, Kasemo B, Käll M, Zou S, Schatz GC. Confined Plasmons in Nanofabricated Single Silver Particle Pairs: Experimental Observations of Strong Interparticle Interactions. *J Phys Chem B*. 2005; 109:1079–1087. [PubMed: 16851063]
80. Romero I, Aizpurua J, Bryant GW, Garcia de Abajo FJ. Plasmons in nearly touching metallic nanoparticles: singular response in the limit of touching dimers. *Opt Express*. 2006; 14:9988–9999. [PubMed: 19529393]
81. Jain PK, Huang W, El-Sayed MA. On the universal scaling behavior of the distance decay of plasmon coupling in metal nanoparticle pairs: a plasmon ruler equation. *Nano Lett*. 2007; 7:2080–2088.
82. Dhawan A, Norton SJ, Gerhold MD, Vo-Dinh T. Comparison of FDTD numerical computations and analytical multipole expansion method for plasmonics-active nanosphere dimers. *Opt Express*. 2009; 17:9688–9703. [PubMed: 19506618]
83. Yang L, Wang H, Yan B, Reinhard BM. Calibration of silver plasmon rulers in the 1– 25 nm separation range: Experimental indications of distinct plasmon coupling regimes. *J Phys Chem C*. 2010; 114:4901–4908.
84. Hill RT, Mock JJ, Hucknall A, Wolter SD, Jokerst NM, Smith DR, Chilkoti A. Plasmon ruler with angstrom length resolution. *ACS Nano*. 2012; 6:9237–9246. [PubMed: 22966857]
85. Elghanian R. Selective Colorimetric Detection of Polynucleotides Based on the Distance-Dependent Optical Properties of Gold Nanoparticles. *Science*. 1997; 277:1078–1081. [PubMed: 9262471]
86. Park S-J, Lazarides AA, Storhoff J, Pesce L, Mirkin CA. The structural characterization of oligonucleotide-modified gold nanoparticle networks formed by DNA hybridization. *J Phys Chem B*. 2004; 108:12375–12380.
87. Sebba DS, Mock JJ, Smith DR, Labean TH, Lazarides AA. Reconfigurable core-satellite nanoassemblies as molecularly-driven plasmonic switches. *Nano Lett*. 2008; 8:1803–1808. [PubMed: 18540653]
88. Maye MM, Kumara MT, Nykypanchuk D, Sherman WB, Gang O. Switching binary states of nanoparticle superlattices and dimer clusters by DNA strands. *Nat Nanotechnol*. 2010; 5:116–120. [PubMed: 20023646]
89. Yan Y, Chen JIL, Ginger DS. Photoswitchable Oligonucleotide-Modified Gold Nanoparticles: Controlling Hybridization Stringency with Photon Dose. *Nano Lett*. 2012

90. Lu Y, Liu Y, Zhang S, Wang S, Zhang S, Zhang X. Aptamer-based plasmonic sensor array for discrimination of proteins and cells with the naked eye. *Anal Chem.* 2013; 85:6571–6574. [PubMed: 23796129]
91. Fong KE, Yung L-YL. Analysis of metallic nanoparticle-DNA assembly formation in bulk solution via localized surface plasmon resonance shift. *RSC Adv.* 2012; 2:5154.
92. Reinhard BM, Sheikholeslami S, Mastroianni A, Alivisatos AP, Liphardt J. Use of plasmon coupling to reveal the dynamics of DNA bending and cleavage by single EcoRV restriction enzymes. *Proc Natl Acad Sci U S A.* 2007; 104:2667–2672. [PubMed: 17307879]
93. Skewis LR, Reinhard BM. Spermidine modulated ribonuclease activity probed by RNA plasmon rulers. *Nano Lett.* 2008; 8:214–220. [PubMed: 18052230]
94. Chen JIL, Durkee H, Traxler B, Ginger DS. Optical Detection of Protein in Complex Media with Plasmonic Nanoparticle Dimers. *Small.* 2011; 7:1993–1997. [PubMed: 21671429]
95. Sannomiya T, Hafner C, Voros J. In situ sensing of single binding events by localized surface plasmon resonance. *Nano Lett.* 2008; 8:3450–3455. [PubMed: 18767880]
96. Waldeisen JR, Wang T, Ross BM, Lee LP. Disassembly of a core-satellite nanoassembled substrate for colorimetric biomolecular detection. *ACS Nano.* 2011; 5:5383–5389. [PubMed: 21667984]
97. Tokarev I, Tokareva I, Minko S. Optical nanosensor platform operating in near-physiological pH range via polymer-brush-mediated plasmon coupling. *ACS Appl Mater Interfaces.* 2011; 3:143–146. [PubMed: 21275381]
98. Tokareva I, Minko S, Fendler JH, Hutter E. Nanosensors based on responsive polymer brushes and gold nanoparticle enhanced transmission surface plasmon resonance spectroscopy. *J Am Chem Soc.* 2004; 126:15950–15951. [PubMed: 15584714]
99. Agrawal A, Deo R, Wang GD, Wang MD, Nie S. Nanometer-scale mapping and single-molecule detection with color-coded nanoparticle probes. *Proc Natl Acad Sci U S A.* 2008; 105:3298–3303. [PubMed: 18305159]
100. Wu L, Reinhard BM. Probing subdiffraction limit separations with plasmon coupling microscopy: concepts and applications. *Chem Soc Rev.* 2014; 43:3884–3897. [PubMed: 24390574]
101. Yu X, Wang J, Feizpour A, Reinhard BM. Illuminating the lateral organization of cell-surface CD24 and CD44 through plasmon coupling between Au nanoparticle immunolabels. *Anal Chem.* 2013; 85:1290–1294. [PubMed: 23320416]
102. Wang J, Boriskina SV, Wang H, Reinhard BM. Illuminating epidermal growth factor receptor densities on filopodia through plasmon coupling. *ACS Nano.* 2011; 5:6619–6628. [PubMed: 21761914]
103. Mock JJ, Hill RT, Degiron A, Zauscher S, Chilkoti A, Smith DR. Distance-dependent plasmon resonant coupling between a gold nanoparticle and gold film. *Nano Lett.* 2008; 8:2245–2252. [PubMed: 18590340]
104. Hill RT, Mock JJ, Urzhumov Y, Sebba DS, Oldenburg S, Chen S-Y, Lazarides AA, Chilkoti A, Smith DR. Leveraging Nanoscale Plasmonic Modes to Achieve Reproducible Enhancement of Light. *Nano Lett.* 2010; 10:4150–4154. [PubMed: 20804206]
105. Mock JJ, Hill RT, Tsai Y-J, Chilkoti A, Smith DR. Probing dynamically tunable localized surface plasmon resonances of film-coupled nanoparticles by evanescent wave excitation. *Nano Lett.* 2012; 12:1757–1764. [PubMed: 22429053]
106. Ciraci C, Hill RT, Mock JJ, Urzhumov Y, Fernández-Domínguez AI, Maier SA, Pendry JB, Chilkoti A, Smith DR. Probing the ultimate limits of plasmonic enhancement. *Science.* 2012; 337:1072–1074. [PubMed: 22936772]
107. Moreau A, Ciraci C, Mock JJ, Hill RT, Wang Q, Wiley BJ, Chilkoti A, Smith DR. Controlled-reflectance surfaces with film-coupled colloidal nanoantennas. *Nature.* 2012; 492:86–89. [PubMed: 23222613]
108. Hill RT, Kozek KM, Hucknall A, Smith DR, Chilkoti A. Nanoparticle-Film Plasmon Ruler Interrogated with Transmission Visible Spectroscopy. *ACS Photonics.* 2014; 10.1021/ph500190q
109. Chen S, Chien F, Lin G, Lee K. Enhancement of the resolution of surface plasmon resonance biosensors by control of the size and distribution of nanoparticles. *Opt Lett.* 2004; 29:1390–1392. [PubMed: 15233445]



110. He L, Smith E, Natan MJ, Keating CD. The distance-dependence of colloidal Au-amplified surface plasmon resonance. *J Phys Chem B*. 2004; 108:10973–10980.
111. Hutter E, Fendler JH, Roy D. Surface Plasmon Resonance Studies of Gold and Silver Nanoparticles Linked to Gold and Silver Substrates by 2-Aminoethanethiol and 1,6-Hexanedithiol. *J Phys Chem B*. 2001; 105:11159–11168.
112. He L, Musick MD, Nicewarner SR, Salinas FG, Benkovic SJ, Natan MJ, Keating CD. Colloidal Au-enhanced surface plasmon resonance for ultrasensitive detection of DNA hybridization. *J Am Chem Soc*. 2000; 122:9071–9077.
113. Jung J, Na K, Lee J, Kim K-W, Hyun J. Enhanced surface plasmon resonance by Au nanoparticles immobilized on a dielectric SiO<sub>2</sub> layer on a gold surface. *Anal Chim Acta*. 2009; 651:91–97. [PubMed: 19733741]
114. Kang T, Hong S, Choi I, Sung JJ, Kim Y, Hahn J-S, Yi J. Reversible pH-driven conformational switching of tethered superoxide dismutase with gold nanoparticle enhanced surface plasmon resonance spectroscopy. *J Am Chem Soc*. 2006; 128:12870–12878. [PubMed: 17002381]
115. Wang F, Wang J, Liu X, Dong S. Nanoparticle-amplified surface plasmon resonance study of protein conformational change at interface. *Talanta*. 2008; 77:628–634.
116. Jiang G, Baba A, Ikarashi H, Xu R, Locklin J, Kashif K, Shinbo K, Kato K, Kaneko F, Advincula R. Signal enhancement and tuning of surface plasmon resonance in Au nanoparticle/polyelectrolyte ultrathin films. *J Phys Chem C*. 2007; 111:18687–18694.
117. Hong X, Hall EAH. Contribution of gold nanoparticles to the signal amplification in surface plasmon resonance. *Analyst*. 2012; 137:4712–4719. [PubMed: 22950078]
118. Sundaramurthy A, Crozier KB, Kino G, Fromm D, Schuck P, Moerner W. Field enhancement and gap-dependent resonance in a system of two opposing tip-to-tip Au nanotriangles. *Phys Rev B*. 2005; 72:165409.
119. Sun M, Fang Y, Yang Z, Xu H. Chemical and electromagnetic mechanisms of tip-enhanced Raman scattering. *Phys Chem Chem Phys*. 2009; 11:9412. [PubMed: 19830324]
120. Yeo B-S, Stadler J, Schmid T, Zenobi R, Zhang W. Tip-enhanced Raman Spectroscopy – Its status, challenges and future directions. *Chem Phys Lett*. 2009; 472:1–13.
121. Vlcková B, Moskovits M, Pavel I, Sisková K, Sládková M, Slouf M. Single-molecule surface-enhanced Raman spectroscopy from a molecularly-bridged silver nanoparticle dimer. *Chem Phys Lett*. 2008; 455:131–134.
122. Lim D-K, Jeon K-S, Kim HM, Nam J-M, Suh YD. Nanogap-engineerable Raman-active nanodumbbells for single-molecule detection. *Nat Mater*. 2010; 9:60–67. [PubMed: 20010829]
123. Rycenga M, Camargo PHC, Li W, Moran CH, Xia Y. Understanding the SERS Effects of Single Silver Nanoparticles and Their Dimers, One at a Time. *J Phys Chem Lett*. 2010; 1:696–703. [PubMed: 20368749]
124. Moskovits M. Persistent misconceptions regarding SERS. *Phys Chem Chem Phys*. 2013; 15:5301. [PubMed: 23303267]
125. Andreou C, Hoonejani MR, Barmi MR, Moskovits M, Meinhart CD. Rapid detection of drugs of abuse in saliva using surface enhanced Raman spectroscopy and microfluidics. *ACS Nano*. 2013; 7:7157–7164. [PubMed: 23859441]
126. Driskell JD, Primera-Pedrozo OM, Dluhy RA, Zhao Y, Tripp RA. Quantitative surface-enhanced Raman spectroscopy based analysis of microRNA mixtures. *Appl Spectrosc*. 2009; 63:1107–1114. [PubMed: 19843360]
127. Driskell JD, Uhlenkamp J, Lipert RJ, Porter MD. Surface-enhanced Raman scattering immunoassays using a rotated capture substrate. *Anal Chem*. 2007; 79:4141–4148. [PubMed: 17487976]
128. Nie S, Emory S. Probing single molecules and single nanoparticles by surface-enhanced Raman scattering. *Science*. 1997; 275:1102. [PubMed: 9027306]
129. Chen S-Y, Lazarides AA. Quantitative Amplification of Cy5 SERS in ‘Warm Spots’ Created by Plasmonic Coupling in Nanoparticle Assemblies of Controlled Structure. *J Phys Chem C*. 2009; 113:12167–12175.

130. Schwartzberg A, Grant C, Wolcott A, Talley C, Huser T, Bogomolni R, Zhang J. Unique gold nanoparticle aggregates as a highly active surface-enhanced Raman scattering substrate. *J Phys Chem B*. 2004; 108:19191–19197.
131. Imura K, Okamoto H, Hossain M, Kitajima M. Visualization of localized intense optical fields in single gold-nanoparticle assemblies and ultrasensitive Raman active sites. *Nano Lett*. 2006; 6:2173–2176. [PubMed: 17034078]
132. Itoh T, Biju V, Ishikawa M, Kikkawa Y, Hashimoto K, Ikehata A, Ozaki Y. Surface-enhanced resonance Raman scattering and background light emission coupled with plasmon of single Ag nanoaggregates. *J Chem Phys*. 2006; 124:134708. [PubMed: 16613469]
133. Qian X, Peng X, Ansari D, Yin-Goen Q, Chen G, Shin D, Yang L, Young A, Wang MD, Nie S. In vivo tumor targeting and spectroscopic detection with surface-enhanced Raman nanoparticle tags. *Nat Biotechnol*. 2007; 26:83–90. [PubMed: 18157119]
134. Zhang H, Harpster MH, Park HJ, Johnson PA, Wilson WC. Surface-enhanced Raman scattering detection of DNA derived from the west Nile virus genome using magnetic capture of Raman-active gold nanoparticles. *Anal Chem*. 2011; 83:254–260. [PubMed: 21121693]
135. Zhang H, Harpster MH, Wilson WC, Johnson PA. Surface-enhanced Raman scattering detection of DNAs derived from virus genomes using Au-coated paramagnetic nanoparticles. *Langmuir*. 2012; 28:4030–4037. [PubMed: 22276995]
136. Nguyen CT, Nguyen JT, Rutledge S, Zhang J, Wang C, Walker GC. Detection of chronic lymphocytic leukemia cell surface markers using surface enhanced Raman scattering gold nanoparticles. *Cancer Lett*. 2010; 292:91–97. [PubMed: 20042272]
137. Neng J, Harpster MH, Zhang H, Mecham JO, Wilson WC, Johnson PA. A versatile SERS-based immunoassay for immunoglobulin detection using antigen-coated gold nanoparticles and malachite green-conjugated protein A/G. *Biosens Bioelectron*. 2010; 26:1009–1015. [PubMed: 20864330]
138. Ikeda K, Suzuki S, Uosaki K. Crystal face dependent chemical effects in surface-enhanced Raman scattering at atomically defined gold facets. *Nano Lett*. 2011; 11:1716–1722. [PubMed: 21417470]
139. Gehan H, Fillaud L, Chehimi MM, Aubard J, Hohenau A, Felidj N, Mangeney C. Thermo-induced electromagnetic coupling in gold/polymer hybrid plasmonic structures probed by surface-enhanced Raman scattering. *ACS Nano*. 2010; 4:6491–6500. [PubMed: 21028846]
140. Kim NH, Lee SJ, Moskovits M. Aptamer-mediated surface-enhanced Raman spectroscopy intensity amplification. *Nano Lett*. 2010; 10:4181–4185. [PubMed: 20863079]
141. Park W-H, Ahn S-H, Kim ZH. Surface-Enhanced Raman Scattering from a Single Nanoparticle-Plane Junction. *ChemPhysChem*. 2008; 9:2491–2494. [PubMed: 18937223]
142. Braun GB, Lee SJ, Dante M, Nguyen T-Q, Moskovits M, Reich NO. Surface-enhanced Raman spectroscopy for DNA detection by nanoparticle assembly onto smooth metal films. *J Am Chem Soc*. 2007; 129:6378–6379. [PubMed: 17469825]
143. Driskell JD, Lipert RJ, Porter MD. Labeled gold nanoparticles immobilized at smooth metallic substrates: systematic investigation of surface plasmon resonance and surface-enhanced Raman scattering. *J Phys Chem B*. 2006; 110:17444–17451. [PubMed: 16942083]
144. Anderson DJ, Moskovits M. A SERS-active system based on silver nanoparticles tethered to a deposited silver film. *J Phys Chem B*. 2006; 110:13722–13727. [PubMed: 16836316]
145. Kim K, Yoon JK. Raman scattering of 4-aminobenzenethiol sandwiched between Ag/Au nanoparticle and macroscopically smooth Au substrate. *J Phys Chem B*. 2005; 109:20731–20736. [PubMed: 16853687]
146. Daniels JK, Chumanov G. Nanoparticle-mirror sandwich substrates for surface-enhanced Raman scattering. *J Phys Chem B*. 2005; 109:17936–17942. [PubMed: 16853302]
147. Driskell JD, Kwarta K, Lipert RJ, Porter MD, Neill J, Ridpath J. Low-level detection of viral pathogens by a surface-enhanced Raman scattering based immunoassay. *Anal Chem*. 2005; 77:6147–6154. [PubMed: 16194072]
148. Punj D, Ghenuche P, Moparthi SB, De Torres J, Grigoriev V, Rigneault H, Wenger J. Plasmonic antennas and zero-mode waveguides to enhance single molecule fluorescence detection and

fluorescence correlation spectroscopy toward physiological concentrations. *Wiley Interdiscip Rev Nanomed Nanobiotechnol.* 2014; 6:268–282. [PubMed: 24616447]

### Further Reading/Resources

1. Dahlin AB, Wittenberg NJ, Höök F, Oh S-H. Promises and challenges of nanoplasmonic devices for refractometric biosensing. *Nanophotonics.* 2013; 2:1–19.
2. Brolo A. Plasmonics for future biosensors. *Nat Photonics.* 2012; 6:709–713.
3. Anker J, Hall W, Lyandres O, Shah N, Zhao J, Van Duyne RP. Biosensing with plasmonic nanosensors. *Nat Mater.* 2008; 7:442–453. [PubMed: 18497851]

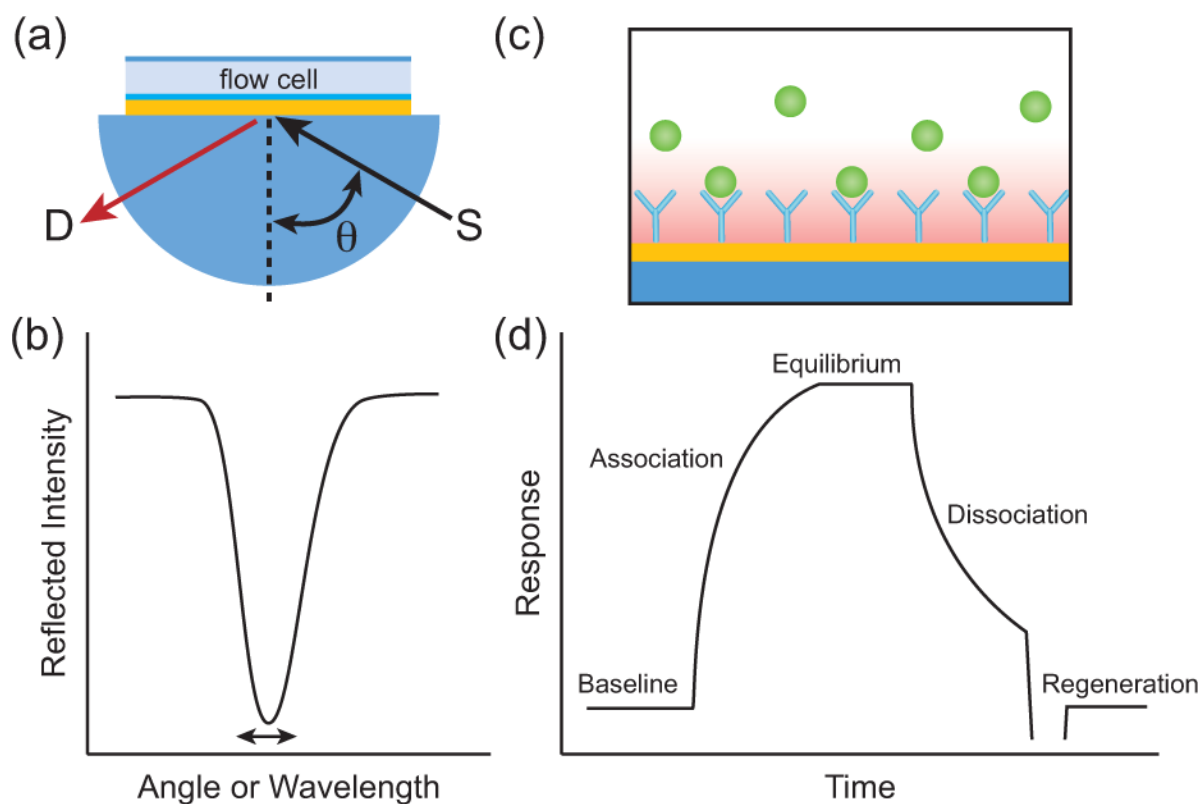


**Figure 1.**

A surface plasmon resonance (SPR) can be excited in thin gold film using the Kretschmann configuration (a, S: Source, D: Detector) and detected as a sharp decrease in the intensity of the reflected beam occurring at the SPR angle or wavelength (b). Film SPR is often used to study biomolecular interactions (c). Target analyte binding by the film-immobilized receptors is detected by a shift in the film SPR. This SPR shift can be monitored over time as target analyte is introduced into the flow cell and then washed away. Kinetic parameters describing the molecular interaction can be calculated from the resulting SPR sensorgram (d, Reproduced with permission from Ref 6. Copyright 2000 Elsevier)

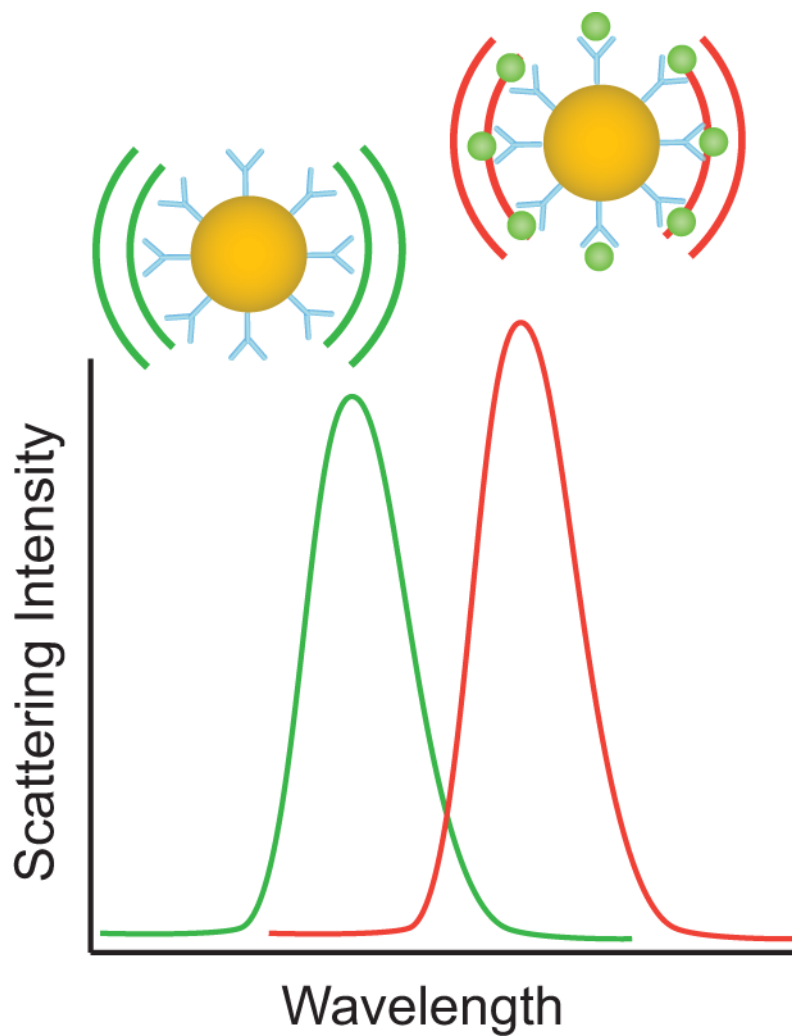


**Figure 2.** Localized surface plasmon resonances (LSPRs) from plasmon resonant nanoparticles (NPs) are sensitive to the refractive index of their surroundings. A plasmon resonant NP functionalized with receptor molecules will display a red shift in the scattering spectrum of its LSPR as it binds target analyte.

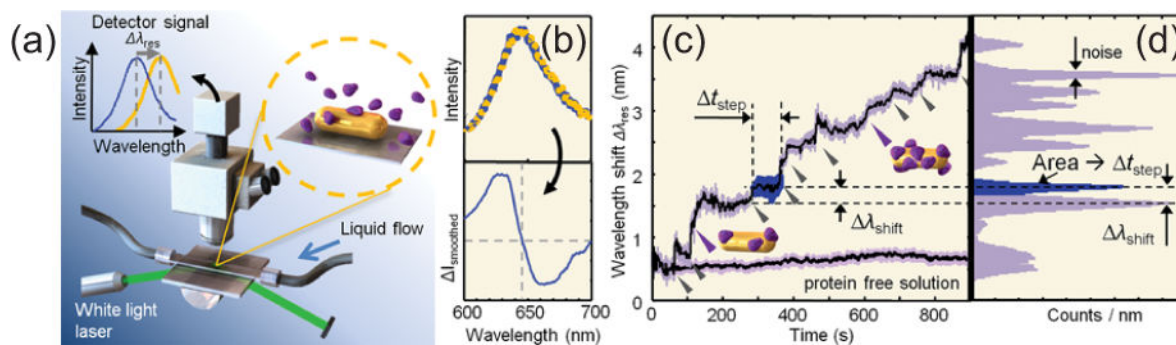


**Figure 3.**

Single nanoparticles (NPs) can be spectroscopically characterized using a dark field microscope (a). The localized surface plasmon resonance (LSPR) of a NP shifts when protein attaches to the surface of the NP (b). This LSPR shift was tracked over time to reveal step-wise attachment of single proteins to the NP being analyzed (c, d). Reprinted with permission from Ref 29. Copyright 2012 ACS.

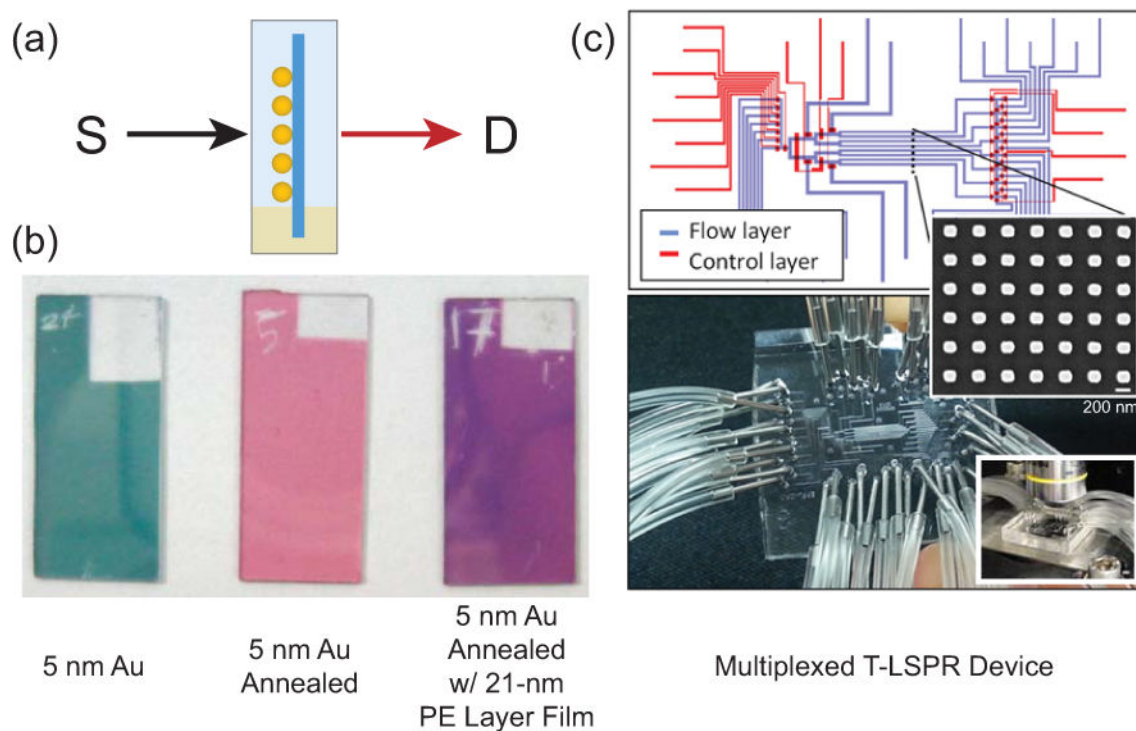


**Figure 4.**

A transmitted localized surface plasmon spectroscopy (T-LSPR) measurement is depicted in (a, S: Source, D: Detector) as an extinction measurement, where the collective LSPR of an ensemble of plasmon resonant nanoparticles (NPs) immobilized on a transparent substrate is measured using a spectrophotometer and a collinear optical path. The photo in (b) gives a visual representation of a simple T-LSPR experiment. Glass slides with immobilized gold nanoisland films show drastic color changes with annealing of the gold coating and addition of polymer layers to the nanoislands (Reprinted with permission from Ref 39. Copyright 2014 ACS) A multiplexed T-LSPR device is shown in (c) that contains microchannels for delivery of solutions to separate T-LSPR sensing arrays (Adapted with permission from Ref 42. Copyright 2014 ACS).

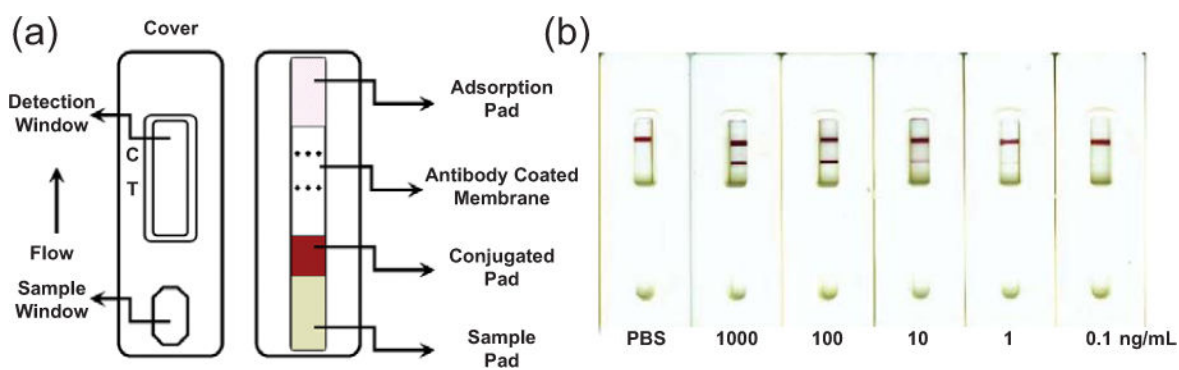


**Figure 5.**

A lateral flow assay using colloidal gold for colorimetric, visual detection is depicted in (a, C: Control, T: Test). The assay demonstrated a qualitative increase in signal in the Test region with increasing target concentration (b). Adapted with permission from Ref. 56. Copyright 2010 Elsevier.



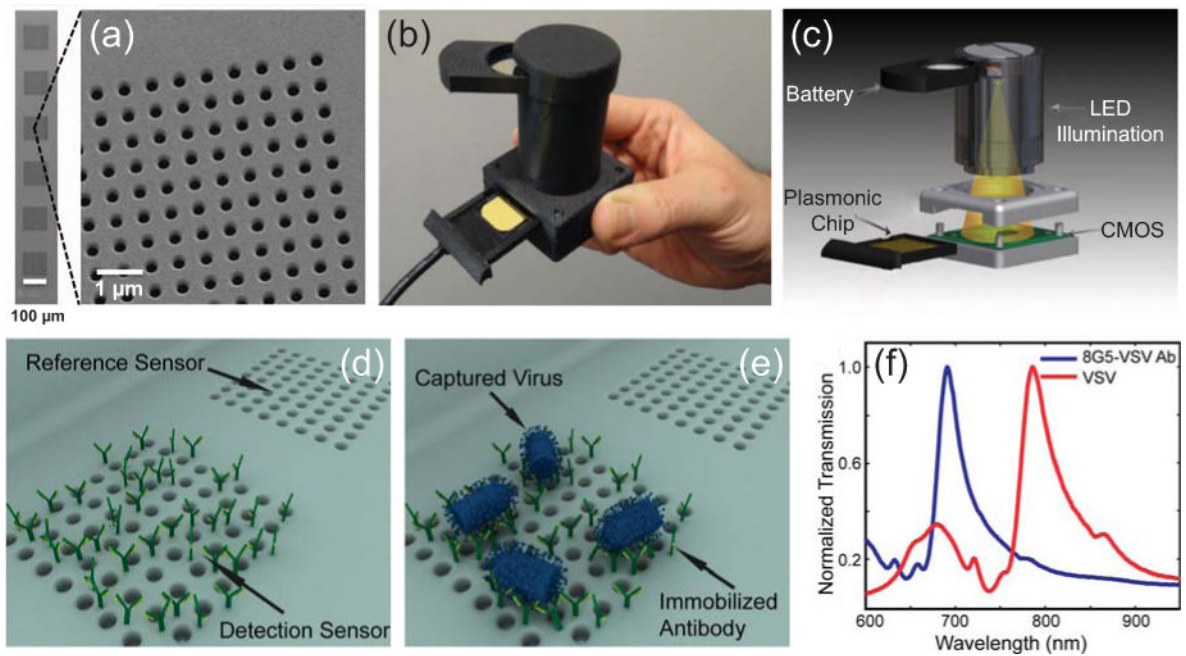


**Figure 6.** Plasmonic nanopores (a) exhibit extraordinary optical transmission (EOT) when illuminated collinearly due to excited plasmonic modes defined by the grating order of the nanopore array. A handheld miniature nanopore array sensing device is shown in (b and c). An example of nanopore sensing is shown in (d–f) where the presence of a virus (red plot) is detected by a shift in the wavelength of the EOT from a nanopore sensing array containing antibodies targeting the virus (blue plot). (a–c) Adapted with permission from Ref 65. Copyright 2014 NPG. (d–f) Adapted with permission from Ref 68. Copyright 2010 ACS.

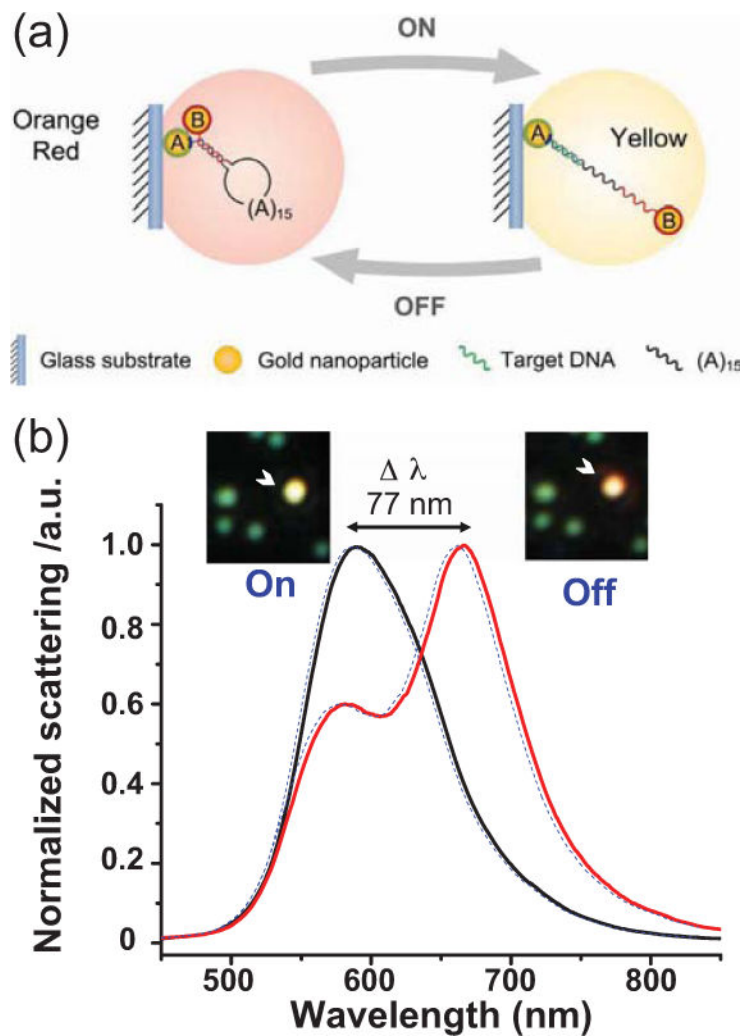


**Figure 7.** A plasmonically coupled nanoparticle (NP) dimer designed to detect DNA is depicted in (a). When target DNA is present the separation distance between the NPs increases and produces a blue shift in the coupled localized surface plasmon resonance of the NP dimer (b). The NP dimer in the inset dark field images (b) is indicated by an arrow. Reproduced with permission from Ref 77. Copyright 2013 Wiley.

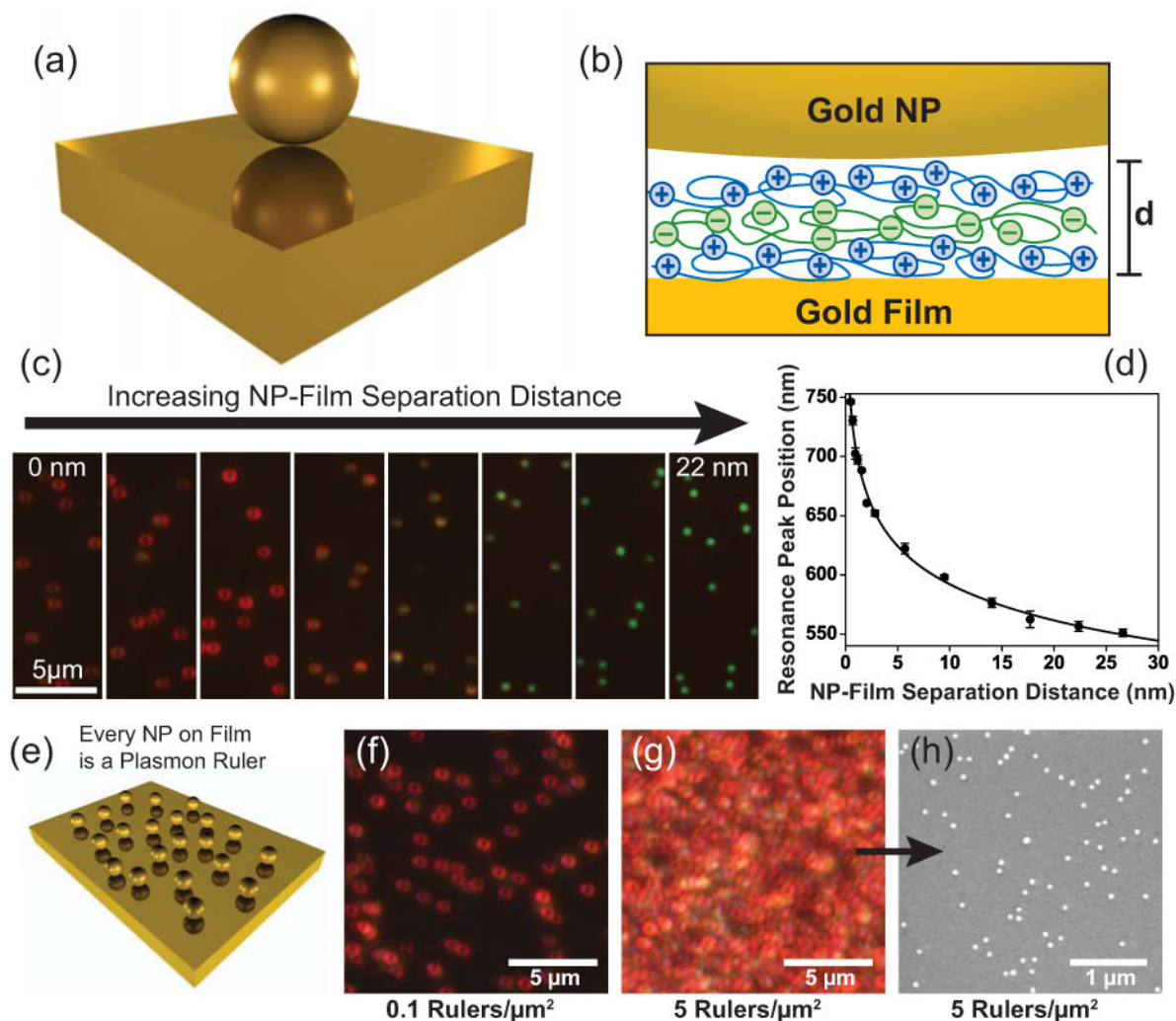


**Figure 8.**

A gold nanoparticle (NP) can become plasmonically coupled to nearby gold film, which can be conceptualized optically by the formation of a virtual NP dimer with one half of the dimer being an effective mirror image of the real NP above the film (a). Molecular spacer layers (b) are used to control the nanoscale separation distance between the NPs and film. As the NP-film separation distance increases a blue shift in the film-coupled NP localized surface plasmon resonance (LSPR) occurs, which is characteristic of a plasmon ruler (c, d). NP-film plasmon rulers are created efficiently with 100% yield (e, f), and so it is possible to create a high density of plasmon rulers over a large surface area (g, h) for characterization with ensemble spectroscopic measurements. Adapted with permission from Refs. <sup>84, 103, 104, and 105</sup>. Copyright 2008, 2010, 2012 ACS.

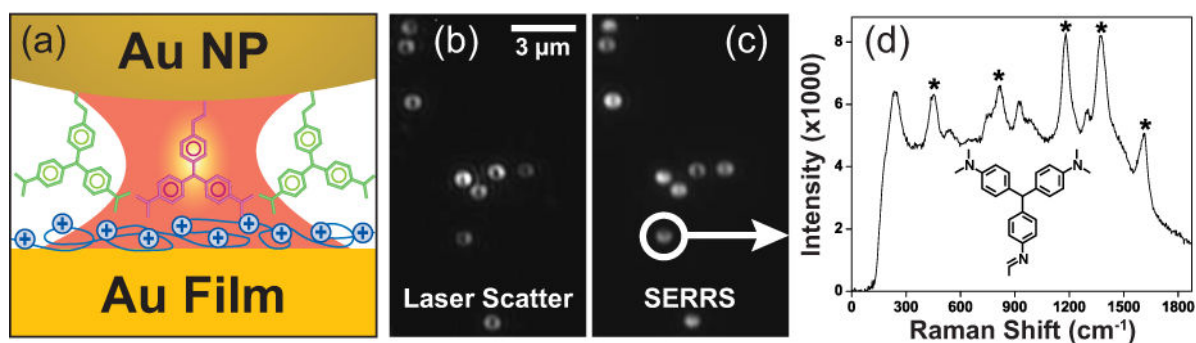


**Figure 9.**

Gold nanoparticles (NPs) in close proximity to gold film create localized regions of field enhancement that can be used for stimulated surface enhanced resonance Raman scattering (SERRS, a). The NP-film SERRS hot spots are generated with 100% yield as is indicated by the fact that each NP in the laser scatter image also appears in the SERRS image (b). A SERRS spectrum with characteristic peaks from a Raman reporter molecule can be collected from each film-coupled NP (c). Adapted with permission from Ref 104. Copyright 2010 ACS.